Model Order Reduction of Parametrized Nonlinear Reaction–Diffusion Systems

Martin A. Grepl[1]

Bericht Nr. 322 **Februar 2011**

Key words: Reaction–diffusion equation, model order reduction, reduced basis approximation, empirical interpolation method, nonlinar systems.

AMS subject classifications: 65M60, 35K57, 35K55

Institut für Geometrie und Praktische Mathematik
RWTH Aachen

Templergraben 55, D–52056 Aachen (Germany)

[1] Numerical Mathematics, RWTH Aachen University, Templergraben 55, 52056 Aachen, Germany.
Email address: grepl@igpm.rwth-aachen.de (Martin A. Grepl)
Tel.: +49 241 8096470, Fax: +49 241 8096470

Model Order Reduction of Parametrized Nonlinear Reaction-Diffusion Systems

Martin A. Grepl[1]

RWTH Aachen University, Numerical Mathematics, Templergraben 55, 52056 Aachen, Germany

Abstract

We present a model order reduction technique for parametrized nonlinear reaction-diffusion systems. In our approach we combine the reduced basis method — a computational framework for rapid evaluation of functional outputs associated with the solution of parametrized partial differential equations — with the empirical interpolation method — a tool to construct "affine" coefficient-function approximations of nonlinear parameter dependent functions. We develop an efficient offline-online computational procedure for the evaluation of the reduced basis approximation: in the offline stage, we generate the reduced basis space; in the online stage, given a new parameter value, we calculate the reduced basis output. The operation count for the online stage depends only on the dimension of the reduced order model and the parametric complexity of the problem. The method is thus ideally suited for the many-query or real-time contexts. We present numerical results for a non-isothermal reaction-diffusion model to confirm and test our approach.

Email address: grepl@igpm.rwth-aachen.de (Martin A. Grepl)

[1]Tel.: +49 241 8096470, Fax: +49 241 80696470

Keywords: Reaction-Diffusion Equation, Model Order Reduction, Reduced Basis Approximation, Empirical Interpolation Method, Nonlinear Systems

1. Introduction

Nonlinear reaction-diffusion systems appear in a large number of real-world applications: ranging from Biology, to Ecology, to Physiology, to Chemistry (Smoller, 1994). Inherent to these equations and the specific application area are a large number of parameters – such as reaction rates or diffusion coefficients — which, in general, have a very strong influence on the dynamic behavior of the system. To analyze and understand the specific problem, many different parameter combinations have to be investigated. The solution of reaction-diffusion systems, however, is a very challenging task because the equations are time-dependent, often highly nonlinear, and coupled. Efficient solution techniques which can characterize many parameter combinations are therefore important. Furthermore, in many applications — such as chemical engineering — understanding, modeling, and simulation is often only the first step; the actual goal is the design, optimization, or real-time control of the problem of interest. Model order reduction techniques are vital in achieving these goals, see e.g. (Marquardt, 2002; Shvartsman et al., 2000; Christofides, 2001a,b) and (Shvartsman & Kevrekidis, 1998; Balsa-Canto et al., 2004).

In this paper we propose a model order reduction technique for nonlinear reaction-diffusion systems whose general formulation is given by

$$\frac{\partial \mathbf{y}(x,t;\mu)}{\partial t} = \nabla \left(D(\mu)\mathbf{y}(x,t;\mu) \right) + \mathbf{f}(\mathbf{y}(x,t;\mu);\mu), \tag{1}$$

where $x \in \Omega \subset R^d$ is the spatial domain, $\mu \in \mathcal{D}$ is the parameter vector, $\mathbf{y}$ is the vector-valued field variable, e.g., containing temperatures and concentrations, $D(\mu)$ is the diffusion matrix, and $\mathbf{f}(\mathbf{y};\mu)$ is a vector-valued function containing the (non)linear reaction terms. Our particular application is the self-ignition of a coal stockpile with Arrhenius type nonlinearity (Brooks et al., 1988a). We note, however, that similar models are also used in combustion theory, biology, and in the description of porous catalysts.

Many model-order reduction (MOR) techniques for linear and nonlinear time-dependent systems are proposed in the literature: the most well-known are proper orthogonal decomposition (POD or Karhunen-Loève decomposition) (Sirovich & Kirby, 1987; Sirovich, 1987; Holmes et al., 1996), balanced truncation (Moore, 1981), and various related hybrid (Lall et al., 1999, 2002; Hahn & Edgar, 2002; Willcox & Peraire, 2001; Rowley, 2005) techniques. It is important to note, however, that most MOR techniques focus mainly on reduced-order modeling of dynamical systems in which time is considered the *only* "parameter;" the development of reduced-order models for problems with a simultaneous dependence of the field variable on parameter and time — our focus here — is much less common (see (Bui et al., 2003; Christensen et al., 2000; Daniel et al., 2002; Gunzburger et al., 2007) for a few exceptions). Furthermore, it is well known that most MOR techniques for nonlinear systems do not result in computational savings compared to the underlying high-dimensional model despite the often significant dimension reduction (Rathinam & Petzold, 2003). Two approaches to resolve this issue have been proposed previously in (Astrid, 2004) and (Romijn et al., 2008).

Our goal is the development of a model order reduction technique for cou-

pled nonlinear reaction-diffusion systems that permits (i) the simultaneous dependence of the field variable (and output) on both time and parameters, and (ii) an efficient offline-online computational procedure which results in significant computational savings when solving the reduced system. To achieve these goals we pursue the reduced basis method (Prud'homme et al., 2002); see (Rozza et al., 2008) for a review of contributions to the methodology. In the recent past, reduced basis approximations and associated *a posteriori* error estimation procedures have been developed for many problems ranging from linear elliptic to nonlinear time-dependent problems: e.g. the steady and unsteady Navier-Stokes equations are considered in (Veroy & Patera, 2005; Knezevic et al., submitted 2009), linear time-dependent convection-diffusion equations in (Grepl & Patera, 2005; Haasdonk & Ohlberger, 2008), steady and unsteady viscous Burgers equation in (Veroy et al., 2003; Nguyen et al., 2009), and nonlinear elliptic and parabolic problems in (Grepl et al., 2007; Grepl, submitted, 2010).

This paper is organized as follows: In Section 2 we provide a review of the reduced basis method for parametrized nonlinear dynamic systems. In Section 3 we extend the methodology to treat nonlinear reaction-diffusion systems. As a specific example, we consider a model for the self-ignition of a coal stockpile with Arrhenius type nonlinearity. Numerical results showing the performance of our model order reduction technique are presented in Section 4. We offer concluding remarks in Section 5.

2. Methodology

We present a review of the reduced basis method for scalar parametrized nonlinear dynamic systems. The presentation of this section is as follows: first, we introduce an abstract problem statement; we then introduce the empirical interpolation method for constructing a coefficient-function approximation of the nonlinear term; finally, we develop the reduced basis approximation for nonlinear parabolic problems and discuss computational complexity.

2.1. Problem Formulation

Our focus here is on nonlinear parabolic partial differential equations (PDEs) with parametric dependence. The reduced basis approximation is based on the weak formulation of the governing equation. We therefore state the general abstract formulation and subsequently present a concrete example: a nonlinear reaction-diffusion equation with Arrhenius type nonlinearity.

For simplicity, we directly consider a time-discrete framework associated to the time interval $I \equiv]0, t_f]$ ($\bar{I} \equiv [0, t_f]$). We divide $\bar{I}$ into K subintervals of equal length $\Delta t = \frac{t_f}{K}$ and define $t^k \equiv k\Delta t$, $0 \leq k \leq K \equiv \frac{t_f}{\Delta t}$; for notational convenience, we also introduce $\mathbb{K} \equiv \{1, \ldots, K\}$. We shall consider Euler-Backward for the time integration; we can also readily treat higher-order schemes such as Crank-Nicolson (Grepl, 2005).

The abstract formulation can be stated as follows: given a parameter $\mu \in \mathcal{D} \subset \mathbb{R}^P$, the field variable $y^{\mathrm{e}}(x, t^k; \mu) \in Y^{\mathrm{e}}$, $\forall k \in \mathbb{K}$, satisfies the weak

form of the μ-parametrized parabolic PDE

$$m(y^{\mathrm{e}}(t^k;\mu),v) + \Delta t\; a(y^{\mathrm{e}}(t^k;\mu),v;\mu) + \Delta t \int_\Omega g(y^{\mathrm{e}}(t^k;\mu);x;\mu)\, v \\ = m(y^{\mathrm{e}}(t^{k-1};\mu),v) + \Delta t\; b(v)\; u(t^k),\;\; \forall v \in Y^{\mathrm{e}},\;\; \forall k \in \mathbb{K}, \quad (2)$$

with initial condition (say) $y^{\mathrm{e}}(x,t^0;\mu) = 0$. Here, $\mathcal{D}$ is the parameter domain in which our P-tuple (input) parameter μ resides; Y^{e} is an appropriate Hilbert space; and $\Omega \subset \mathbb{R}^d$ is our spatial domain, a point in which shall be denoted x. Furthermore, $b(\cdot)$ and $a(\cdot,\cdot;\mu)$, $m(\cdot,\cdot)$ are continuous bounded linear and bilinear forms, respectively; $u(t^k)$ denotes the "control input" at time $t = t^k$; and $g(w;x;\mu)$ is a nonlinear function continuous in its arguments. We assume here that $b(\cdot)$, and $m(\cdot,\cdot)$ do not depend on the parameter; parameter dependence, however, is readily admitted (Grepl & Patera, 2005). We note that if an explicit scheme such as Euler-Forward is used, we then arrive at a linear system for $y^{\mathrm{e}}(t^k;\mu)$ but now burdened with a conditional stability restriction on Δt. In that case, the discrete reduced basis system will also be inheritedly linear.

In general, we are not interested in the field variable – such as temperature – at all points in Ω per se, but rather at specific performance metrics or outputs – such as averaged temperatures or heat fluxes – of the system. These outputs are typically functionals of the field variable: given the solution $y^{\mathrm{e}}(x,t^k;\mu) \in Y^{\mathrm{e}}$, $\forall k \in \mathbb{K}$, of (2), we evaluate the (here, single) output of interest from

$$s^{\mathrm{e}}(t^k;\mu) = \ell(y^{\mathrm{e}}(t^k;\mu)), \quad \forall k \in \mathbb{K}, \quad (3)$$

where $\ell(\cdot)$ is a linear bounded functional.

The superscript e denotes the "exact" — more precisely, semi-discrete —

problem. In actual practice, of course, we do not have access to the exact solution; we thus replace the exact solution with a reference (or "truth") approximation, which resides in (say) a suitably fine piecewise-linear finite element approximation space $Y \subset Y^{\rm e}$ of *very* large dimension $\mathcal{N}$. We associated to Y a set of piecewise linear (over each element) basis functions $\phi_i(x),\ 1 \le i \le \mathcal{N}$. Our "truth" finite element approximation $y^k(\mu) \equiv y(t^k;\mu) \in Y$ to the semi-discrete problem (2) is then given by

$$m(y^k(\mu),v) + \Delta t\ a(y^k(\mu),v;\mu) + \Delta t \int_\Omega g(y^k(\mu);x;\mu)\, v \\ = m(y^{k-1}(\mu),v) + \Delta t\ b(v)\ u(t^k),\ \forall v \in Y,\ \forall k \in \mathbb{K}, \quad (4)$$

with initial condition $y(t^0;\mu) = 0$; we then evaluate the output $s^k(\mu) \equiv s(t^k;\mu) \in \mathbb{R}$ from

$$s^k(\mu) = \ell(y^k(\mu)), \quad \forall k \in \mathbb{K}. \quad (5)$$

Note that in the sequel we will drop the explicity dependence on the spatial variable x and use the notation $y^k(\mu) = y(x,t^k;\mu)$ unless the x-dependence is essential. We shall assume — hence the appellation "truth" — that the discretization is sufficiently rich such that $y^k(\mu)$ and $y^{\rm e}(t^k;\mu)$ and hence $s^k(\mu)$ and $s^{\rm e}(t^k;\mu)$ are indistinguishable. The reduced-basis approximation shall be built upon our reference finite element approximation, and the reduced-basis error will thus be evaluated with respect to $y^k(\mu) \in Y$.

We shall further assume that the bilinear form a depends affinely on the parameter μ and can be expressed as

$$a(w,v;\mu) = \sum_{q=1}^{Q_a} \Theta_a^q(\mu)\ a^q(w,v), \quad \forall w,v \in Y,\ \forall \mu \in \mathcal{D}, \quad (6)$$

for some (preferably) small integer Q_a. Here, the function $\Theta_a^q(\mu) : \mathcal{D} \rightarrow \mathbb{R}$ depends on μ, but the continuous form a^q does *not* depend on μ. We note that the assumption of affine parameter dependence (6) holds for many problems with both property (i.e. physical) and geometry parametric variations (Rozza et al., 2008).

We also briefly recall the algebraic equations induced by (4) and (5). We expand $y^k(\mu) = \sum_{n=1}^{\mathcal{N}} \phi_j(x) y_j^k(\mu)$, then $\underline{y}^k(\mu) = [y_1^k(\mu) \dots y_{\mathcal{N}}^k(\mu)]^T \in \mathbb{R}^{\mathcal{N}}$ satisfies

$$(M + \Delta t\, A(\mu))\, \underline{y}^k(\mu) + \Delta t\, F(\underline{y}^k(\mu); \mu) = M\, \underline{y}^{k-1}(\mu) + \Delta t\, B\, u(t^k),\ \forall k \in \mathbb{K} \quad (7)$$

with initial condition $\underline{y}^0(\mu) = 0$; we then evaluate the output from

$$s^k(\mu) = L^T \underline{y}^k(\mu), \quad \forall k \in \mathbb{K}. \quad (8)$$

The elements of the mass and stiffness matrices $M \in \mathbb{R}^{\mathcal{N}\times\mathcal{N}}$ and $A(\mu) \in \mathbb{R}^{\mathcal{N}\times\mathcal{N}}$ are given by $M_{i,j} = m(\phi_j, \phi_i),\ 1 \le i, j \le \mathcal{N}$ and $A_{i,j}(\mu) = a(\phi_j, \phi_i; \mu)$, $1 \le i, j \le \mathcal{N}$, respectively; the elements of the nonlinear term are given by $F_i(\underline{y}^k(\mu); \mu) = \int_\Omega g(y^k(\mu); x; \mu)\, \phi_i,\ 1 \le i \le \mathcal{N}$; and the elements of the load vector $B \in \mathbb{R}^{\mathcal{N}}$ are given by $B_i = b(\phi_i),\ 1 \le i \le \mathcal{N}$.

Example 1 (*A nonlinear reaction diffusion problem*). We consider a single one-step reaction of a reacting mixture in the region $\Omega = [0, 1]$. The combustion model is given by the PDE (Adjerid & Flaherty, 1986; Kapila, 1983)

$$\frac{\partial T(x,t)}{\partial t} = \alpha \frac{\partial^2 T(x,t)}{\partial x^2} + D\,(1 - T(x,t))\, e^{-\gamma/(T(x,t)+1)} \quad (9)$$

with initial condition $T(x, t = 0) = 0$ and boundary conditions $T(x = 0, t) = T(x = 1, t) = 0$. Here, $T(x, t)$ is the temperature at position x and time t, α

is the thermal diffusivity, D is the Damköhler number, and γ is the activation energy.

The governing equation (9) depends on three parameters; we may thus define the input parameter vector $\mu = [\mu_1, \mu_2, \mu_3] \equiv [\alpha, D, \gamma]$. We next derive the weak formulation of (9) and discretize in time using Euler-Backward and in space using finite elements. The equation then assumes the form (4) with $m(w, v) = \int w\, v\, d\Omega$, $a(w, v; \mu) = \alpha \int \frac{\partial w}{\partial x} \frac{\partial v}{\partial x}\, d\Omega$, $b(v) = 0$, and the nonlinearity is given by $g(w; \mu) = D\,(1 - w)\, e^{-\gamma/(w+1)}$. We note that $a(w, v; \mu)$ trivially satisfies the affine parameter dependence with $Q_a = 1$: $\Theta_a^1(\mu) = \alpha$ and $a^1(w, v) = \int \frac{\partial w}{\partial x} \frac{\partial v}{\partial x}\, d\Omega$.

2.2. Empirical Interpolation Method

The empirical interpolation method (EIM), introduced in (Barrault et al., 2004), serves to construct affine approximations of parameter dependent non-affine or nonlinear functions. The method is frequently applied in reduced basis approximations of parametrized partial differential equations (Grepl et al., 2007); an affine approximation of the operator allows an efficient "offline-online" computational procedure and is thus crucial for efficiency (see Section 2.3.2).

2.2.1. Function Interpolation

The EIM approximation space, W_M^g, is – in essence – spanned by pre-computed snapshots of the nonlinear parameter dependent function. Given W_M^g, we construct an approximation to the nonlinear function as a linear combination of the EIM basis functions. The particular linear combination is determined through interpolation at the EIM interpolation nodes

$T_M^g = \{x_1^g, x_2^g, \ldots, x_M^g\}$, a set of judiciously selected points in the spatial domain. The construction of W_M^g and T_M^g is based on a greedy selection process. We present the procedure described in (Grepl, submitted, 2010); see (Maday et al., 2009) for the linear nonaffine case.

We first introduce a finite train sample $\Xi_{\text{train}} \subset \mathcal{D}$ of size $|\Xi_{\text{train}}|$ which shall serve as our computational surrogate for $\mathcal{D}$. We also require the function $\text{POD}_{L^2(\Omega)}(\{w^k(\mu), 1 \le k \le K\})$, which returns the largest POD mode, χ_1, with respect to the $(\cdot,\cdot)_{L^2(\Omega)}$ inner product. Here, $L^2(\Omega)$ is the space of square integrable functions over Ω. We use the method of snapshots to obtain χ_1 (Sirovich, 1987): to this end, we solve the eigenvalue problem $C\psi^i = \lambda^i \psi^i$ for $(\psi^1 \in \mathbb{R}^K, \lambda^1 \in \mathbb{R})$ associated with the largest eigenvalue of C, where $C_{ij} = (w^i(\mu), w^j(\mu))_{L^2(\Omega)},\ 1 \le i, j \le K$; we then obtain the first POD mode from $\chi_1 = \sum_{k=1}^K \psi_k^1 \, w^k(\mu)$.

The POD/Greedy-EIM procedure proceeds by induction: we first choose randomly an initial parameter value $\mu_1 \in \mathcal{D}$ and perform a POD of the time-history of the nonlinear function to obtain the POD mode $\xi_1(x) = \text{POD}_{L^2(\Omega)}(\{g(y^k(x;\mu_1);x;\mu_1), 1 \le k \le K\})$. We define the first EIM interpolation node as $x_1^g \equiv \arg\sup_{x\in\Omega} |\xi_1(x)|$ and the first EIM basis function as $q_1(x) \equiv \xi_1(x)/\xi_1(x_1^g)$; we further define the EIM space $W_1^g = \text{span}\{q_1\}$. We also introduce a nodal value matrix B^1 with a single element $B_{1,1}^1 = q_1(x_1^g) = 1$.

Next, for $1 \le M \le M_{\max} - 1$, we compute for all $\mu \in \Xi_{\text{train}}$ the empirical interpolation of $g(y^k(x;\mu);x;\mu),\ \forall k \in \mathbb{K}$: we first solve the linear system

$$\sum_{j=1}^{M} B_{i\,j}^M \varphi_{M\,j}^k(\mu) = g(y^k(x_i^g;\mu);x_i^g;\mu), \quad 1 \le i \le M,\ \forall k \in \mathbb{K}, \tag{10}$$

and compute the empirical interpolation $g_M^{y^k}(x;\mu) \in W_M^g,\ \forall k \in \mathbb{K}$, as

$$g_M^{y^k}(x;\mu) = \sum_{i=1}^{M} \varphi_{M\,i}^k(\mu)\, q_i(x). \tag{11}$$

We choose the next parameter as the maximizer of the $L^\infty(\Omega)$ EIM interpolation error over Ξ_{train} summed over time,

$$\mu_{M+1} = \arg\max_{\mu\in\Xi_{\text{train}}} \sum_{k=1}^{K} \|g(y^k(x;\mu);x;\mu) - g_M^{y^k}(x;\mu)\|_{L^\infty(\Omega)}. \tag{12}$$

Given μ_{M+1}, we perform a POD of the time-history of the interpolation error to obtain $\xi_{M+1}(x) = \text{POD}_{L^2(\Omega)}(\{e_{M,\text{EIM}}^k(\mu_{M+1}), 1 \le k \le K\})$, where $e_{M,\text{EIM}}^k(\mu) = g(y^k(\mu_{M+1});x;\mu_{M+1}) - g_M^{y^k}(x;\mu_{M+1}),\ \forall k \in \mathbb{K}$. Note that we perform a POD on the interpolation error instead of the nonlinear function itself in order to consistently "add" new information at each step of the POD/Greedy procedure.

To generate the interpolation points we first solve the linear system $\sum_{j=1}^M \sigma_j^M\, q_j(x_i^g) = \xi_{M+1}(x_i^g),\ 1 \le i \le M$, and we set $r_{M+1}(x) \equiv \xi_M(x) - \sum_{j=1}^M \sigma_j\, q_j(x)$. We then define the interpolation point

$$x_{M+1}^g \equiv \arg\sup_{x\in\Omega} |r_{M+1}(x)|, \tag{13}$$

the next EIM basis function as

$$q_{M+1}(x) \equiv r_{M+1}(x)/r_{M+1}(x_{M+1}^g); \tag{14}$$

and expand the EIM space

$$W_{M+1}^g \leftarrow W_M^g \cup \text{span}\{q_{M+1}(x)\}. \tag{15}$$

Finally, we define the nodal value matrix $B^{M+1} \in \mathbb{R}^{(M+1)\times(M+1)}$,

$$B^{M+1}_{i,j} = q_j(x^g_i), \quad 1 \le i, j \le M+1. \tag{16}$$

Note that by construction, B^M, $1 \le M \le M_{\max}$, is lower triangular and hence computation of the EIM coefficients $\varphi^k_{M\,j}$ in (10) is an $\mathcal{O}(M^2)$ operation per timestep. It can be shown that the interpolation process is well-defined. For more details on the EIM including an a priori and a posteriori error analysis for the linear nonaffine case we refer the interested reader to (Grepl et al., 2007; Barrault et al., 2004; Maday et al., 2009; Eftang et al., 2010).

In general, we may also specify a desired error tolerance, $\epsilon_{\text{tol,min}}$, and stop the procedure as soon as $\max_{\mu\in\Xi_{\text{train}}} \sum_{k=1}^{K} \|g(y^k(x;\mu);x;\mu) - g^{y^k}_M(x;\mu)\|_{L^\infty(\Omega)} \le \epsilon_{\text{tol,min}}$ is satisfied; $M_{\max}$ is then indirectly determined through the stopping criterion. We also note that we require the truth solution for all μ in Ξ_{train} to generate the EIM interpolation points and space. There is thus a trade-off concerning the size of Ξ_{train}, i.e., the training sample should be chosen large enough to capture the essential dynamics of the system but as small as possible to limit the computational burden to generate the EIM space.

2.3. Reduced Basis Method

The critical observation of the reduced basis method is that the field variable $y^k(\mu)$, $\forall k \in \mathbb{K}$, is not, in fact, some arbitrary member of the very high dimensional finite element space Y; rather, it resides, or "evolves," on a much lower dimensional manifold — in effect, a $P+1$ dimensional manifold — induced by the parametric and temporal dependence. Thus, by restricting our attention to this manifold, we can adequately approximate the field variable by a space of dimension $N \ll \mathcal{N}$.

2.3.1. Approximation

We suppose that we are given the nested reduced basis spaces

$$W_N^y = \text{span}\{\zeta_n,\ 1 \le n \le N\}, \quad 1 \le N \le N_{\max}, \tag{17}$$

where the $\zeta_n,\ 1 \le n \le N$, are mutually orthogonal basis functions. We comment on the adaptive procedure for constructing the basis functions in Section 2.3.3.

Given the nested EIM space $W_M^g = \text{span}\{q_1, \ldots, q_M\},\ 1 \le M \le M_{\max}$ and nested set of interpolation points $T_M^g = \{x_1^g, \ldots, x_M^g\},\ 1 \le M \le M_{\max}$, our reduced basis approximation $y_{N,M}^k(\mu)$ to $y^k(\mu)$ is obtained by a standard Galerkin projection: given $\mu \in \mathcal{D}$, $y_{N,M}^k(\mu) \in W_N^y$ satisfies

$$\begin{aligned} m(y_{N,M}^k(\mu), v) + \Delta t\ a(y_{N,M}^k(\mu), v; \mu) + \Delta t \int_\Omega g_M^{y_{N,M}^k}(x;\mu)\ v \\ = m(y_{N,M}^{k-1}(\mu), v) + \Delta t\, b(v)\, u(t^k), \quad \forall v \in W_N^y,\ \forall k \in \mathbb{K}, \end{aligned} \tag{18}$$

with initial condition $y_{N,M}^0(\mu) = 0$. We then evaluate the output approximation, $s_{N,M}^k(\mu) \in \mathbb{R}$, from

$$s_{N,M}^k(\mu) = \ell(y_{N,M}^k(\mu)), \quad \forall k \in \mathbb{K}. \tag{19}$$

Here, $g_M^{y_{N,M}^k}(x;\mu) \in W_M^g$ is given by

$$g_M^{y_{N,M}^k}(x;\mu) = \sum_{i=1}^M \tilde{\varphi}_{M\,i}^k(\mu)\, q_i(x). \tag{20}$$

where the coefficients $\tilde{\varphi}_{M\,i}^k(\mu),\ 1 \le i \le M$, are the solution of the linear system

$$\sum_{j=1}^M B_{ij}^M \tilde{\varphi}_{M\,j}^k(\mu) = g(y_{N,M}^k(x_i^g;\mu); x_i^g; \mu), \quad 1 \le i \le M,\ \forall k \in \mathbb{K}. \tag{21}$$

Note that the space W_M^g is constructed based on $g(y^k(\mu); x; \mu)$ and not $g(y_{N,M}^k(\mu); x; \mu)$. However, as N and M increase the reduced basis solution $y_{N,M}^k(\mu)$ converges to the truth solution $y^k(\mu)$ very rapidly. We thus expect $g(y_{N,M}^k(\mu); x; \mu)$ to be well approximated in W_M^g. We shall observe the (in fact, exponential) convergence when we discuss numerical results in Section 4.

At this point we emphasize the need to incorporate the empirical interpolation method into the reduced basis approximation. If we were to follow the classical approach, the term $\int_\Omega g_M^{y_{N,M}^k}(x; \mu)\ v$ in (18) would be replace by $\int_\Omega g(y_N^k(x; \mu); x; \mu)\ v$. Despite the (presumably) low dimension N of the reduced basis space, the computational complexity to evaluate the latter term depends on the dimension $\mathcal{N}$ of the underlying truth approximation. This is the reason why most model order reduction techniques for nonlinear problem do not result in computational savings compared to the underlying high-dimensional approximation (Rathinam & Petzold, 2003). The EIM allows us to completely decouple the evaluation of the reduced basis approximation from the truth approximation; we discuss the computational procedure in the next section. We also note that other approaches to resolve this problem have been proposed previously, see e.g. (Astrid, 2004; Romijn et al., 2008). Recently, the EIM has also been applied in combination with the Proper Orthogonal Decomposition in (Chaturantabut & Sorensen, 2010).

Finally, we note that the need to incorporate the empirical interpolation method into the reduced basis approximation only exists for high-order polynomial or non-polynomial nonlinearities (Grepl et al., 2007). If g is a low-order (or at most quadratically) polynomial nonlinearity in $y^k(\mu)$, we can

expand the nonlinear terms into their power series and develop an efficient, i.e., online $\mathcal{N}$-independent, offline-online computational decomposition using the standard Galerkin procedure (Veroy & Patera, 2005; Veroy et al., 2003).

2.3.2. Computational Procedure

We summarize here the offline-online computational procedure in order to fully exploit the dimension reduction of the problem and to recover online $\mathcal{N}$-independence even in the nonlinear case. We first express $y^k_{N,M}(\mu)$ as

$$y^k_{N,M}(\mu) = \sum_{n=1}^{N} y^k_{N,Mn}(\mu)\ \zeta_n, \tag{22}$$

and choose as test functions $v = \zeta_j,\ 1 \le j \le N$, in (18). It then follows from the affine representation (20) of $g_M^{y^k_{N,M}}$ that the reduced basis approximation $\underline{y}^k_{N,M}(\mu) = [y^k_{N,M\,1}(\mu)\ \ y^k_{N,M\,2}(\mu)\ \ \dots\ \ y^k_{N,M\,N}(\mu)]^T \in \mathbb{R}^N$, satisfies

$$\begin{aligned}(M_N + \Delta t\ A_N(\mu))\ \underline{y}^k_{N,M}(\mu) + \Delta t\ C^{N,M}\ \underline{\tilde{\varphi}}^k_M(\mu)& \\ = M_N\ \underline{y}^{k-1}_{N,M}(\mu) + \Delta t\ B_N\ u(t^k),\ \forall k \in \mathbb{K},&\end{aligned} \tag{23}$$

with initial condition $y^0_{N,M\,n}(\mu) = 0,\ 1 \le n \le N$, and the coefficients $\underline{\tilde{\varphi}}^k_M(\mu) = [\tilde{\varphi}^k_{M\,1}(\mu)\ \tilde{\varphi}^k_{M\,2}(\mu)\ \dots\ \tilde{\varphi}^k_{M\,M}(\mu)]^T \in \mathbb{R}^M,\ \forall k \in \mathbb{K}$, are determined from (21).

We next define the matrix $Z = [\zeta_1\ \zeta_2 \dots \zeta_N] \in \mathbb{R}^{\mathcal{N}\times N}$ containing the reduced basis vectors and the matrix $Z_q = [q_1\ q_2 \dots q_M] \in \mathbb{R}^{\mathcal{N}\times M}$ containing the EIM basis vectors. Given the finite element mass matrix M, stiffness matrix $A(\mu)$, load vector B, and output vector L defined in Section 2.1, we can directly derive the reduced basis quantities: the *parameter independent* matrices $M_N \in \mathbb{R}^{N\times N}$ and $C^{N,M} \in \mathbb{R}^{N\times M}$ are given by $M_N = Z^T M Z$ and

$C^{N,M} = Z^T M Z_q$, respectively; $B_N \in \mathbb{R}^N$ is a *parameter independent* vector given by $B_N = Z^T B$; and $A_N(\mu) \in \mathbb{R}^{N\times N}$ is a parameter dependent matrix given by $A_N(\mu) = Z^T A(\mu) Z$. Invoking the affine decomposition (6) we obtain

$$A_N(\mu) = \sum_{q=1}^{Q_a} \Theta_a^q(\mu)\ A_N^q, \tag{24}$$

where the *parameter independent* quantities $A_N^q \in \mathbb{R}^{N\times N}$ are given by

$$A_N^q = Z^T\, A^q\, Z, \quad 1 \le q \le Q_a. \tag{25}$$

We can now substitute $\underline{\tilde{\varphi}}^k_{M\,m}(\mu)$ from (21) into (23) to obtain the nonlinear algebraic system

$$\begin{aligned}(M_N + \Delta t\ A_N(\mu))\ \underline{y}^k_{N,M}(\mu) + \Delta t\ D^{N,M}\ g(Z^{N,M}\,\underline{y}^k_{N,M}(\mu); \underline{x}^g_M; \mu)& \\ = M_N\ \underline{y}^{k-1}_{N,M}(\mu) + \Delta t\, B_N\, u(t^k), \quad \forall\, k \in \mathbb{K},&\end{aligned} \tag{26}$$

where $D^{N,M} = C^{N,M}(B^M)^{-1} \in \mathbb{R}^{N\times M}$, $Z^{N,M} \in \mathbb{R}^{M\times N}$ is a *parameter-independent* matrix with entries $Z^{N,M}_{i,j} = \zeta_j(x^g_i),\ 1 \le i \le M,\ 1 \le j \le N$;and $\underline{x}^g_M = [x^g_i\ \ldots x^g_M]^T \in \mathbb{R}^M$ is the set of interpolation points. We now solve for $\underline{y}^k_{N,M}(\mu)$ at each timestep using a Newton iterative scheme: given the solution for the previous timestep, $\underline{y}^{k-1}_{N,M}(\mu)$, and a current iterate $\bar{\underline{y}}^k_{N,M}(\mu)$, we find an increment $\delta\underline{y}_{N,M}$ such that

$$\begin{aligned}&\left(M_N + \Delta t\ A_N(\mu) + \Delta t \bar{E}^N\right)\ \delta\underline{y}_{N,M} \\ &\quad = M_N\ \underline{y}^{k-1}_{N,M}(\mu) + \Delta t\ B_N(\mu)\ u(t^k) - (M_N + \Delta t\ A_N(\mu))\ \bar{\underline{y}}^k_{N,M}(\mu) \\ &\qquad\qquad - \Delta t\ D^{N,M}\ g(Z^{N,M}\,\bar{\underline{y}}^k_{N,M}(\mu); \underline{t}_M; \mu),\end{aligned} \tag{27}$$

where $\bar{E}^N \in \mathbb{R}^{N\times N}$ must be calculated at every Newton iteration from

$$\bar{E}^N_{i,j} = \sum_{m=1}^{M} D^{N,M}_{i,m} g_1\left(\sum_{n=1}^{N} \bar{y}^k_{N,Mn}(\mu)\zeta_n(x^g_m); x^g_m; \mu\right) \zeta_j(x^g_m), \quad 1 \le i,j \le N, \tag{28}$$

and g_1 is the partial derivative of g with respect to the first argument. Finally, we evaluate the output estimate from

$$s^k_{N,M}(\mu) = L^T_N \, \underline{y}^k_{N,M}(\mu), \quad \forall\, k \in \mathbb{K}, \tag{29}$$

where $L_N \in \mathbb{R}^N$ is the output vector given by $L_N = Z^T L$.

The offline-online decomposition is now clear. In the offline stage — performed only *once* — we first construct the nested approximation spaces W^g_M and sets of interpolation points T^g_M, $1 \le M \le M_{\max}$; we then solve for the ζ_n, $1 \le n \le N_{\max}$ and compute and store the μ-independent quantities M_N, B^M, $D^{N,M}$, B_N, $Z^{N,M}$, and A^q_N, $1 \le q \le Q_a$. In the online stage — performed many times, for each new parameter value μ — we first assemble $A_N(\mu)$ from (24); this requires $O(Q_a N^2)$ operations. We then solve (27) for $\underline{y}^k_{N,M}(\mu)$ and evaluate the output estimate $s^k_{N,M}(\mu)$ from (29). The operation count is dominated by the Newton update at each timestep: we first assemble $\bar{E}^N$ from (28) at cost $O(MN^2)$ — note that we perform the sum in the parenthesis of (28) first before performing the outer sum — and then invert the left hand side of (27) at cost $O(N^3)$. The operation count in the online stage is thus $O(Q_a N^2)$ once plus $O(MN^2 + N^3)$ per Newton iteration per timestep. Finally, given $\underline{y}^k_{N,M}(\mu)$ we evaluate the output estimate $s^k_{N,M}(\mu)$, $\forall k \in \mathbb{K}$, from (29) at a cost of $O(KN)$. We thus recover $\mathcal{N}$-independence in the online stage.

Thus, as required in the many-query or real-time contexts, the online

complexity is *independent* of $\mathcal{N}$, the dimension of the underlying "truth" finite element approximation space. Since $N \ll \mathcal{N}$ we expect significant computational savings in the online stage relative to classical discretization and solution approaches.

2.3.3. Adaptive Sampling Procedure

Given W_M^g, T_M^g, and B^M, we invoke a POD/Greedy sampling procedure — a combination of the Proper Orthogonal Decomposition (POD) in time with a Greedy selection procedure in parameter space — to generate W_N^y (Haasdonk & Ohlberger, 2008; Grepl, submitted, 2010). We shall use the "best" possible approximation $g_M^{y_{N,M}^k}(x;\mu)$ of $g(y_{N,M}^k;x;\mu)$ during the sampling process so as to minimize the error induced by the empirical interpolation procedure, i.e., we set $M = M_{\max}$.

We let $\mathrm{POD}_X(\{w^k(\mu), 1 \le k \le K\})$ return the largest POD mode, χ_1, but this time with respect to the $(\cdot,\cdot)_X$ inner product. We define $(\cdot,\cdot)_X = a(\cdot,\cdot;\mu_{\mathrm{ref}})$ for a reference parameter value $\mu_{\mathrm{ref}} \in \mathcal{D}$ (Grepl, submitted, 2010). We again use the method of snapshots to obtain χ_1 (Sirovich, 1987): we solve the eigenvalue problem $C\psi^i = \lambda^i\psi^i$ for $(\psi^1 \in \mathbb{R}^K, \lambda^1 \in \mathbb{R})$ associated with the largest eigenvalue of C, where $C_{ij} = (w^i(\mu), w^j(\mu))_X,\ 1 \le i,j \le K$; we then obtain the first POD mode from $\chi_1 = \sum_{k=1}^K \psi_k^1\, w^k(\mu)$.

The POD/Greedy procedure proceeds as follows: we first choose a $\mu_1 \in \mathcal{D}$ and set $W_0^y = \{0\}$ and $N = 0$. Then, for $1 \le N \le N_{\max}$, we first compute the projection error $e_{N,\mathrm{proj}}^k(\mu_N) = y^k(\mu_N) - \mathrm{proj}_{X,W_{N-1}^y}(y^k(\mu_N))$, $\forall k \in \mathbb{K}$, where $\mathrm{proj}_{X,W_N}(w)$ denotes the X-orthogonal projection of $w \in X$ onto W_N^y, and we expand the reduced basis space $W_N^y \leftarrow W_{N-1}^y \cup \mathrm{POD}_X(\{e_{N,\mathrm{proj}}^k(\mu_N),\ 1 \le k \le K\})$. Finally, we choose the next parameter value from $\mu_{N+1} = \arg\max_{\mu\in\Xi_{\mathrm{train}}}$

$|||y^K(\mu) - y^K_{N,M}(\mu)|||/|||y^K(\mu)|||$, i.e., we perform a greedy search over Ξ_{train} for the largest relative error at the final time. Here, the energy norm is defined as $|||w^k|||^2 = m(w^k, w^k) + \sum_{k'=1}^{k} a(w^{k'}, w^{k'}; \mu)$.

In general, we may also specify a desired error tolerance, $\epsilon_{\text{tol,min}}$, and stop the procedure as soon as $\max_{\mu \in \Xi_{\text{train}}} |||y^K(\mu) - y^K_{N,M}(\mu)|||/|||y^K(\mu)||| \leq \epsilon_{\text{tol,min}}$ is satisfied; $N_{\max}$ is then indirectly determined through the stopping criterion.

3. Nonlinear Reaction-Diffusion Systems

In this section we consider a specific problem belonging to the class of nonlinear reaction-diffusion systems (Smoller, 1994). Reaction-diffusion systems appear in a large number of real-world applications: ranging from Biology, where reaction-diffusion equations characterize the pattern formation in morphogenesis and mutations in genetics; to Ecology, where they govern predator-prey relation and the spreading of epidemics; to Physiology, where the conduction in nerves and carbon monoxide poisoning is described by reaction-diffusion equations; to Chemistry, probably the most notable application area of reaction-diffusion equations. Furthermore, inherent to these equations and the specific application area are a large number of parameters, which, in general, have a very strong influence on the dynamic behavior of the system, e.g., such as reaction rates in chemistry. The reduced basis method is thus ideally suited for the treatment of parametrized nonlinear reaction-diffusion systems.

We now extend the methodology introduced in the last section to coupled systems of nonlinear equations. We introduced separate reduced basis spaces for each field variable. Furthermore, we employ the EIM to generate an

affine approximation of the nonlinear coupling term, thus allowing an efficient offline-online procedure even for the coupled system of nonlinear equations.

3.1. Model Problem

As a specific example, we consider a one-dimensional non-isothermal reaction-diffusion model for the self-ignition of a coal stockpile with Arrhenius type nonlinearity (Schmal et al., 1985; Brooks & Glasser, 1986; Brooks et al., 1988b,a; Salinger et al., 1994). In practice this problem arises if large piles of coal are stored, e.g., in harbors, over extended periods of time. As the oxygen in the air reacts with the coal, the pile starts to heat up and can eventually self-ignite if certain conditions — on porosity, oxygen concentration, and coal size — are met. We also note that similar models are used in combustion theory (see Example 1), biology, and in the description of porous catalysts.

The field variables are the temperature of the reactive medium (here, the coal) normalized by the ambient temperature, $T(x,t) = (\overline{T}(x,t) - \overline{T}_\infty)/\overline{T}_\infty$, and the concentration of the reactantd (here, the oxygen in the air) normalized by the concentration of oxygen in the ambient air, $c(x,t) = (\overline{c}(x,t) - \overline{c}_\infty)/\overline{c}_\infty$. The coupled set of governing equations are given by

$$\frac{\partial T(x,t)}{\partial t} = \nabla^2 T(x,t) + \beta\,\Phi^2\,(c(x,t)+1)\,e^{-\gamma/(T(x,t)+1)}, \tag{30}$$

$$\frac{\partial c(x,t)}{\partial t} = \mathrm{Le}\,\nabla^2 c(x,t) - \Phi^2\,(c(x,t)+1)\,e^{-\gamma/(T(x,t)+1)}, \tag{31}$$

with initial conditions

$$T(x,t=0) = T_0 = 0, \tag{32}$$

$$c(x,t=0) = c_0 = \frac{1}{(3x+1)^2} - 1. \tag{33}$$

The boundary conditions are

$$\begin{aligned} T(x,t)|_{x=0} &= 0, \qquad & T(x,t)|_{x=1} &= 0, \\ c(x,t)|_{x=0} &= 0, \qquad & \left.\frac{\partial c(x,t)}{\partial x}\right|_{x=1} &= 0. \end{aligned} \tag{34}$$

A sketch of the distribution of temperature and concentration for $t > 0$ is shown in Figure 1. Here, $x \in \Omega \subset \mathbb{R}^1$ is the spatial coordinate and $\Omega \equiv [0, 1]$ is the spatial domain. Note that $x = 0$ corresponds to the top of the pile at which $T(x, t)$ and $c(x, t)$ are equal to the the ambient temperature and concentration, respectively; and $x = 1$ corresponds to the bottom of the pile at which $T(x, t)$ is equal to the ground (ambient) temperature, and the concentration gradient is zero. The one-dimensional model accounts only for the vertical variation in the state variable; the length and width of the coal pile are assumed to be much larger than its height. The outputs of interest, s_1 and s_2, are the temperature and concentration at $x = 0.2$ both shifted by one, respectively.

The parameters governing the dynamic behavior of the system are the Arrhenius number, γ, the Prater temperature, β, the Lewis number, Le, and the Thiele modulus, Φ. Note that the Thiele modulus is related to the maximum possible temperature of the system: the temperature satisfies $1 \leq T \leq 1 + \beta$ for Dirichlet boundary conditions and Le $= 1$. Here, we assume that three of those parameters — β, Le, and Φ — are fixed and only γ is varying. The values, taken from (Brooks et al., 1988a), are given by $\beta = 4.287$, $\Phi^2 = 70000$, and Le $= 0.233$; and γ varies in the range $12 \leq \gamma \leq 12.6$. We can thus identify the input parameter $\mu \equiv \gamma \in \mathcal{D} \equiv [12, 12.6] \subset \mathbb{R}^{P=1}$. We will see that the system exhibits a very interesting dynamical behavior in terms of complex oscillatory patterns for this parameter range.

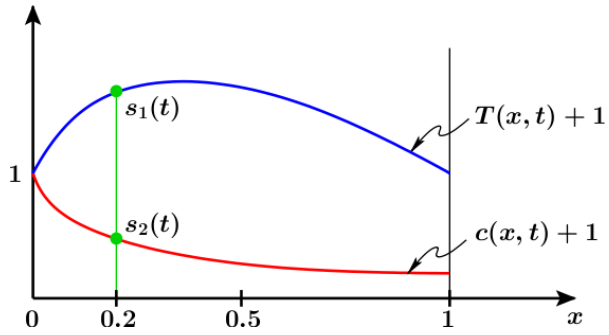

Figure 1: Sketch of temperature distribution and concentration for the model problem for $t > 0$ (Note that both quantities are shifted by 1).

3.2. Truth Approximation

We next derive the weak form of the governing equations (30) and (31) and discretize in time using Euler-Backward. We also introduce the linear finite element truth approximation subspaces $Y_T \equiv \{v | v \in H^1(\Omega), v = 0|_{x=0,1}\}$ and $Y_c \equiv \{v | v \in H^1(\Omega), v = 0|_{x=0}\}$ both of dimension $\mathcal{N} = 501$, where $H^1(\Omega)$ is a suitable Hilbert space and $\Omega \equiv [0, 1]$ is the spatial domain. We associated to Y_T and Y_c a set of piecewise linear (over each element) basis functions $\phi_i(x),\ 1 \le i \le \mathcal{N}$ (note that we use the same spatial discretization for Y_T and Y_c and they thus share the same basis). We shall consider the time interval $\bar{I} = [0, 6]$ and a timestep $\Delta t = 1\,\mathrm{E}{-3}$; we thus have $K = 6000$. Our truth approximation is thus: Given $\mu \in \mathcal{D}$, find $T^k(\mu) \in Y_T$ and $c^k(\mu) \in Y_c$ such that[2]

$$m(T^k(\mu), v_T) + \Delta t\, a(T^k(\mu), v_T) - \Delta t\, \beta\, \Phi^2 \int_\Omega (c^k(\mu) + 1)\, e^{-\mu/(T^k(\mu)+1)}\, v_T = m(T^{k-1}(\mu), v_T), \quad \forall v_T \in Y_T,\ \forall k \in \mathbb{K} \quad (35)$$

[2]Note that we use our usual notation here: $T^k(\mu) = T(x, t^k; \mu)$ and $c^k(\mu) = c(x, t^k; \mu)$.

$$m(c^k(\mu), v_c) + \Delta t\, \mathrm{Le}\, a(c^k(\mu), v_c) + \Delta t\, \Phi^2 \int_\Omega (c^k(\mu) + 1)\, e^{-\mu/(T^k(\mu)+1)}\, v_c$$
$$= m(c^{k-1}(\mu), v_c), \quad \forall v_c \in Y_c,\ \forall k \in \mathbb{K} \quad (36)$$

with inital conditions $m(T^0(\mu), v_T) = m(T_0, v_T),\ \forall v_T \in Y_T,\ m(c^0(\mu), v_c) = m(c_0, v_c),\ \forall v_c \in Y_c$. We then evaluate the outputs from

$$s_1^k(\mu) = \ell(T^k(\mu)) + 1, \qquad \forall k \in \mathbb{K}, \quad (37)$$

and

$$s_2^k(\mu) = \ell(c^k(\mu)) + 1, \quad \forall k \in \mathbb{K}. \quad (38)$$

Here, $\ell(v) = \int_\Omega \delta(x - 0.2)\, v$, where $\delta(x)$ is the Dirac delta function, and the bilinear forms are given by

$$m(w, v) = \int_\Omega w\, v, \quad a(w, v) = \int_\Omega \frac{\partial w}{\partial x}\, \frac{\partial v}{\partial x}. \quad (39)$$

We also define the nonlinearity g as

$$g(c^k(\mu), T^k(\mu); \mu) = (c^k(\mu) + 1)\, e^{-\mu/(T^k(\mu)+1)}. \quad (40)$$

3.2.1. Algebraic Equations

We first expand $T^k(\mu) = \sum_{n=1}^{\mathcal{N}} \phi_n\, T_n^k(\mu)$ and $c^k(\mu) = \sum_{n=1}^{\mathcal{N}} \phi_n\, c_n^k(\mu)$, and choose as test functions $v_T = \phi_n,\ 1 \le n \le \mathcal{N}$ in (35), and $v_c = \phi_n,\ 1 \le n \le \mathcal{N}$ in (36). It then follows that $\underline{T}^k(\mu) = [T_1^k(\mu) \dots T_{\mathcal{N}}^k(\mu)] \in \mathbb{R}^{\mathcal{N}}$ and $\underline{c}^k(\mu) = [c_1^k(\mu) \dots c_{\mathcal{N}}^k(\mu)], \in \mathbb{R}^{\mathcal{N}}$ satisfy

$$M\, \underline{T}^k(\mu) + \Delta t\, A\, \underline{T}^k(\mu)$$
$$- \Delta t\, \beta\, \Phi^2 F(\underline{c}^k(\mu), \underline{T}^k(\mu), \mu) = M\, \underline{T}^{k-1}(\mu), \quad \forall\, k \in \mathbb{K} \quad (41)$$

and

$$M\,\underline{c}^k(\mu) + \Delta t\,\mathrm{Le}\,A\,\underline{c}^k(\mu) + \Delta t\,\Phi^2 F(\underline{c}^k(\mu), \underline{T}^k(\mu), \mu) = M\,\underline{c}^{k-1}(\mu), \quad \forall\, k \in \mathbb{K} \quad (42)$$

with inital conditions $M\,\underline{T}^0(\mu) = \underline{T}_0$, and $M\,\underline{c}^0(\mu) = \underline{c}_0$, respectively. We then evaluate the outputs from

$$s_1^k(\mu) = L^T\,\underline{T}^k(\mu) + 1, \quad \forall k \in \mathbb{K}. \quad (43)$$

and

$$s_2^k(\mu) = L^T\,\underline{c}^k(\mu) + 1, \quad \forall k \in \mathbb{K}. \quad (44)$$

Note that the coupled system of equations (41) and (42) has to be solved for $\underline{T}^k(\mu)$ and $\underline{c}^k(\mu)$ at each timestep using a Newton iterative scheme.

The elemens of the initial condition vectors $\underline{T}_0 \in \mathbb{R}^{\mathcal{N}}$ and $\underline{c}_0 \in \mathbb{R}^{\mathcal{N}}$ are given by $\underline{T}_{0,i} = m(T_0, \phi_i),\ 1 \le i \le \mathcal{N}$, and $\underline{c}_{0,i} = m(c_0, \phi_i),\ 1 \le i \le \mathcal{N}$, respetively. The elements of the mass and stiffness matrices $M \in \mathbb{R}^{\mathcal{N}\times\mathcal{N}}$ and $A \in \mathbb{R}^{\mathcal{N}\times\mathcal{N}}$ are given by $M_{i,j} = m(\phi_j, \phi_i),\ 1 \le i, j \le \mathcal{N}$ and $A_{i,j} = a(\phi_j, \phi_i)$, $1 \le i, j \le \mathcal{N}$, respectively; the elements of the nonlinear term are given by $F_i(\underline{c}^k(\mu), \underline{T}^k(\mu); \mu) = \int_\Omega (c^k(\mu) + 1)\, e^{-\mu/(T^k(\mu)+1)}\, \phi_i,\ 1 \le i \le \mathcal{N}$; and the elements of the output vector $L \in \mathbb{R}^{\mathcal{N}}$ are given by $L_i = \ell(\phi_i),\ 1 \le i \le \mathcal{N}$.

3.2.2. Numerical Results

We present results for the truth approximation. In Figure 2, we plot the outputs s_1 and s_2 for $\mu = 12.0$ over (discrete) time. The sharp peak in the temperature output s_1 and corresponding drop in the concentration output s_2 indicates the ignition of the system. After the ignition, the system goes

into a stable steady-state solution. In Figure 3 we show the corresponding output plots for $\mu = 12.5$; we first note that the ignition occurs at a later point in time and that the maximum temperature reached is higher. For this parameter value the system does not return to a steady-state solution, but converges to a period 1 limit cycle. Finally, we present in Figure 4 the output plots for $\mu = 12.58$. Again, the time of ignition occurs later and the maximum temperature is higher than before. Furthermore, the system converges to a limit cycle with mixed mode oscillations. To clearly visualize the limit cycles, we show in Figures 5 and 6 the phase plots for the solutions corresponding to the two parameter values $\mu = 12.5$ and $\mu = 12.58$ without the transient behavior, respectively. We can clearly see the period 1 limit cycle for $\mu = 12.5$; as μ is increased, a period doubling cascade occurs leading to the mixed mode oscillations for $\mu = 12.58$.

The systems clearly exhibits a very complex dynamic behaviour with a strong dependence on the parameter μ. Approximating such a systems with a reduced order model over parameter and time is certainly a very challenging task.

3.3. Reduced Basis Approximation

We develop the reduced basis approximation for the coupled system of nonlinear equations (35) and (36) by generalizing the approach described in Section 2.3.1. We first introduce a finite train sample $\Xi_{\text{train}} \subset \mathcal{D}$ and solve and store the solutions $T^k(\mu)$ and $c^k(\mu)$ to (35) and (36) for all $\mu \in \Xi_{\text{train}}$ and for all $k \in \mathbb{K}$, respectively. Given $g(c^k(\mu), T^k(\mu); \mu)$ in (40), we generate the nested EIM spaces $W_M^g = \text{span}\{q_1, \ldots, q_M\},\ 1 \leq M \leq M_{\max}$, and nested set of interpolation points $T_M^g = \{x_1^g, \ldots, x_M^g\},\ 1 \leq M \leq M_{\max}$, according to

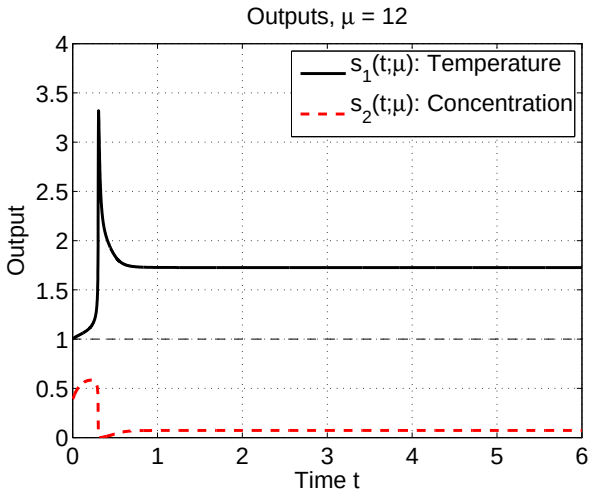

Figure 2: Outputs $s_1(t;\mu)$ and $s_2(t;\mu)$ for $\mu = 12.0$ as a function of time.

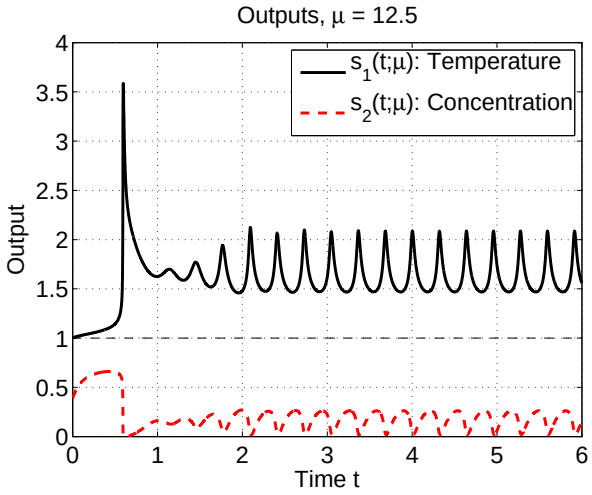

Figure 3: Outputs $s_1(t;\mu)$ and $s_2(t;\mu)$ for $\mu = 12.5$ as a function of time.

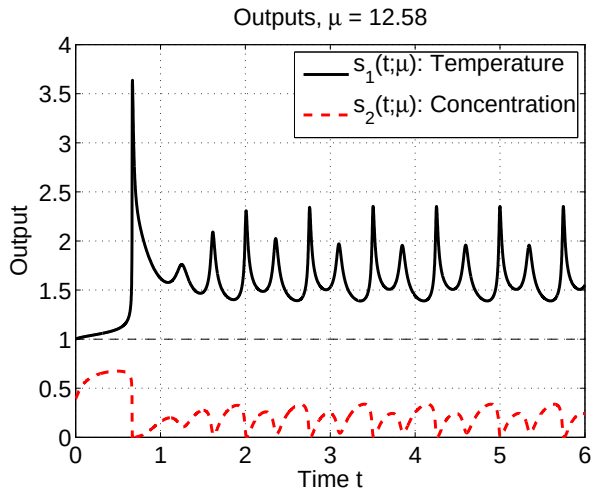

Figure 4: Outputs $s_1(t;\mu)$ and $s_2(t;\mu)$ for $\mu = 12.58$ as a function of time.

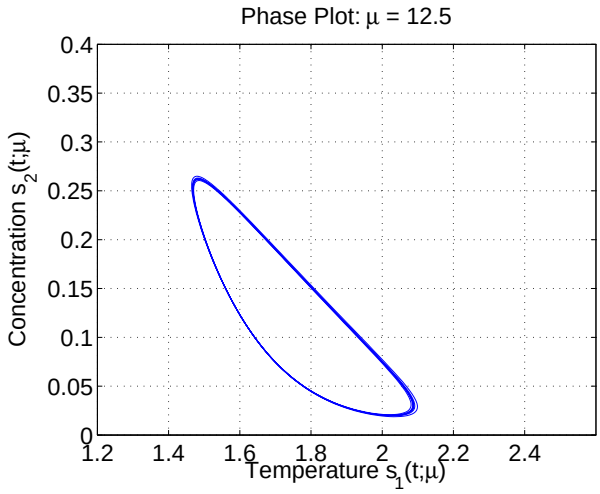

Figure 5: Limit Cycls in phase plane ($s_1(t;\mu)$ vs. $s_2(t;\mu)$) for $\mu = 12.5$ without transition from initial condition.

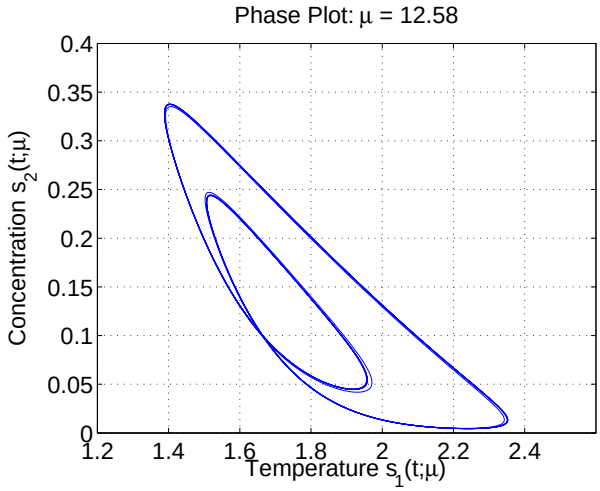

Figure 6: Limit Cycles in phase plane ($s_1(t;\mu)$ vs. $s_2(t;\mu)$) for $\mu = 12.58$ without transition from initial condition.

the procedure described in Section 2.2.1. Note that the nonlinearity depends on both field variables and we thus have to generalize the definition of the interpolant (8) and of the EIM coefficients (7): the approximation $g_M^{c^k,T^k}(x;\mu)$ to $g(c^k(\mu),T^k(\mu);\mu)$ is given by

$$g_M^{c^k,T^k}(x;\mu) = \sum_{m=1}^{M} \varphi_{Mm}^k(\mu) q_m(x) \tag{45}$$

where the coefficients $\varphi_{Mm}^k(\mu)$ are determined from

$$\sum_{j=1}^{M} B_{ij}^M \varphi_{Mj}^k(\mu) = g(c^k(x_i^g;\mu),T^k(x_i^g;\mu);\mu), \quad 1 \le i \le M \tag{46}$$

and $B_{ij}^M = q_j(x_i^g)$, $1 \le i,j \le M$, $1 \le M \le M_{\max}$. Given W_M^g and T_M^g, we next define the associated nested reduced-basis spaces for the temperature

$$W_{N_T}^T = \text{span}\{\zeta_{T,m},\ 1 \le n \le N_T\}, \quad 1 \le N_T \le N_{T,\max}, \tag{47}$$

and the concentration

$$W_{N_c}^c = \text{span}\{\zeta_{c,m},\ 1 \le n \le N_c\}, \quad 1 \le N_c \le N_{c,\max}, \tag{48}$$

according to the adaptive procedure described in Section 2.3.3. We introduce separate spaces for temperature and concentration with possibly different dimensions N_T and N_c, respectively.

Our reduced-basis approximation is then: given $\mu \in \mathcal{D}$, $T_{N,M}^k(\mu) \in W_{N_T}^T$ and $c_{N,M}^k(\mu) \in W_{N_c}^c$ satisfy

$$m(T_{N,M}^k(\mu), v_T) + \Delta t\, a(T_{N,M}^k(\mu), v_T) - \Delta t\, \beta\, \Phi^2 \int_\Omega g_M^{c_{N,M}^k, T_{N,M}^k}(x;\mu)\, v_T = m(T_{N,M}^{k-1}(\mu), v_T), \quad \forall v_T \in W_{N_T}^T,\ \forall k \in \mathbb{K} \tag{49}$$

$$m(c_{N,M}^k(\mu), v_c) + \Delta t\, \text{Le}\, a(c_{N,M}^k(\mu), v_c) + \Delta t\, \Phi^2 \int_\Omega g_M^{c_{N,M}^k, T_{N,M}^k}(x;\mu)\, v_c = m(c_{N,M}^{k-1}(\mu), v_c), \quad \forall v_c \in W_{N_c}^c,\ \forall k \in \mathbb{K} \tag{50}$$

with inital conditions determined from $m(T_{N,M}^0(\mu), v_T) = m(T_0, v_T),\ \forall\, v_T \in W_{N_T}^T$, and $m(c_{N,M}^0(\mu), v_c) = m(c_0, v_c),\ \forall\, v_c \in W_{N_c}^c$; here, $g_M^{c_{N,M}^k, T_{N,M}^k}(x;\mu)$ is given by

$$g_M^{c_{N,M}^k, T_{N,M}^k}(x;\mu) = \sum_{m=1}^M \tilde{\varphi}_{Mm}^k(\mu) q_m(x) \tag{51}$$

where the coefficients $\tilde{\varphi}_{Mm}^k(\mu)$ are determined from

$$\sum_{j=1}^M B_{ij}^M \tilde{\varphi}_{Mj}^k(\mu) = g(c_{N,M}^k(x_i^g;\mu), T_{N,M}^k(x_i^g;\mu);\mu), \quad 1 \le i \le M, \tag{52}$$

and $B_{ij}^M = q_j(x_i^g)$, $1 \le i, j \le M$, $1 \le M \le M_{\max}$. Finally, we evaluate the outputs from

$$s_{1,N,M}^k(\mu) = \ell(T_{N,M}^k(\mu)) + 1, \quad \forall k \in \mathbb{K}, \tag{53}$$

and

$$s^k_{2,N,M}(\mu) = \ell(c^k_{N,M}(\mu)) + 1, \quad \forall k \in \mathbb{K}. \tag{54}$$

3.4. Computational Procedure

The offline-online procedure follows directly from our previous discussion in Section 2.3.2. We first express

$$T^k_{N,M}(\mu) = \sum_{n=1}^{N_T} \zeta_{T,n}\, T^k_{N,Mn}(\mu), \tag{55}$$

$$c^k_{N,M}(\mu) = \sum_{n=1}^{N_c} \zeta_{c,n}\, c^k_{N,Mn}(\mu), \tag{56}$$

and choose as test functions $v_T = \zeta_{T,n},\ 1 \le n \le N_T$ in (49), and $v_c = \zeta_{c,n},\ 1 \le n \le N_c$ in (50). We also define the matrices $Z_T = [\zeta_{T,1}\, \zeta_{T,2} \ldots \zeta_{T,N_T}] \in \mathbb{R}^{\mathcal{N}\times N_T}$, $Z_T = [\zeta_{c,1}\, \zeta_{c,2} \ldots \zeta_{c,N_c}] \in \mathbb{R}^{\mathcal{N}\times N_c}$, and $Z_q = [q_1\, q_2 \ldots q_M] \in \mathbb{R}^{\mathcal{N}\times M}$.

It then follows that $\underline{T}^k_{N,M}(\mu) = [T^k_{N,M1}(\mu) \ldots T^k_{N,MN_T}(\mu)] \in \mathbb{R}^{N_T}$ satisfies

$$(M_{T,N} + \Delta t\, A_{T,N})\, \underline{T}^k_{N,M}(\mu) - \Delta t\, \beta\, \Phi^2\, C_T^{N,M}\, \underline{\tilde{\varphi}}^k_M(\mu) = M_{T,N}\, \underline{T}^{k-1}_{N,M}(\mu), \quad \forall k \in \mathbb{K}, \tag{57}$$

and $\underline{c}^k_{N,M}(\mu) = [c^k_{N,M1}(\mu) \ldots c^k_{N,MN_c}(\mu)], \in \mathbb{R}^{N_c}$ satisfies

$$(M_{c,N} + \Delta t\, \mathrm{Le}\ A_{c,N})\, \underline{c}^k_{N,M}(\mu) - \Delta t\, \Phi^2\, C_c^{N,M}\, \underline{\tilde{\varphi}}^k_M(\mu) = M_{c,N}\, \underline{c}^{k-1}_{N,M}(\mu), \quad \forall k \in \mathbb{K}, \tag{58}$$

with initial condition $M_{T,N}\, \underline{T}^k_{N,M}(\mu) = (Z_T)^T\, \underline{T}_0$, and $M_{c,N}\, \underline{c}^0_{N,M}(\mu) = (Z_c)^T\, \underline{c}_0$. Here, $\underline{\tilde{\varphi}}^k_M(\mu) \equiv [\tilde{\varphi}^k_{M\,1}(\mu) \ldots \tilde{\varphi}^k_{M\,M}(\mu)] \in \mathbb{R}^M$ is determined from (52), and the *parameter-independent* matrices are given by $M_{T,N} = (Z_T)^T M_T Z_T \in \mathbb{R}^{N_T\times N_T}$, $A_{T,N} = (Z_T)^T A_T Z_T \in \mathbb{R}^{N_T\times N_T}$, $C_T^{N,M} = (Z_T)^T M_T Z_q \in \mathbb{R}^{N_T\times M}$,

$M_{c,N} = (Z_c)^T M_c Z_c \in \mathbb{R}^{N_c \times N_c}$, $A_{c,N} = (Z_c)^T M_c Z_c \in \mathbb{R}^{N_c \times N_c}$, and $C_c^{N,M} = (Z_c)^T M_c Z_q \in \mathbb{R}^{N_c \times M}$.

We can now substitute $\underline{\tilde{\varphi}}_M^k(\mu) \in \mathbb{R}^M$ from (52) into (57) and (58) to obtain the coupled system of nonlinear algebraic equations

$$(M_{T,N} + \Delta t\, A_{T,N})\, \underline{T}_{N,M}^k(\mu) - \Delta t\, \beta\, \Phi^2 D_T^{N,M} g\left(Z_c^{N,M}\, \underline{c}_{N,M}^k(\underline{x}_M^g;\mu), Z_T^{N,M}\, \underline{T}_{N,M}^k(\underline{x}_M^g;\mu);\mu\right) = M_{T,N}\, \underline{T}_{N,M}^{k-1}(\mu), \quad (59)$$

$$(M_{c,N} + \Delta t\, \mathrm{Le}\; A_{c,N})\, \underline{c}_{N,M}^k(\mu) - \Delta t\, \Phi^2 D_c^{N,M} g\left(Z_c^{N,M}\, \underline{c}_{N,M}^k(\underline{x}_M^g;\mu), Z_T^{N,M}\, \underline{T}_{N,M}^k(\underline{x}_M^g;\mu);\mu\right) = M_{c,N}\, \underline{c}_{N,M}^{k-1}(\mu), \quad (60)$$

with initial condition $M_{T,N}\, \underline{T}_{N,M}^k(\mu) = (Z_T)^T\, \underline{T}_0$, and $M_{c,N}\, \underline{c}_{N,M}^0(\mu) = (Z_c)^T\, \underline{c}_0$, which has to be solved using (say) Newton's Method for all $k \in \mathbb{K}$ (see Section 2.3.2). Here, $D_T^{N,M} = C_T^{N,M}(B^M)^{-1} \in \mathbb{R}^{N_T \times M}$ and $D_c^{N,M} = C_c^{N,M}(B^M)^{-1} \in \mathbb{R}^{N_c \times M}$; and $Z_T^{N,M} \in \mathbb{R}^{M \times N_T}$ and $Z_c^{N,M} \in \mathbb{R}^{M \times N_c}$ are *parameter-independent* matrices with entries $Z_{Ti,j}^{N,M} = \zeta_{T,j}(x_i^g),\ 1 \le j \le N_T, 1 \le i \le M$ and $Z_{ci,j}^{N,M} = \zeta_{c,j}(x_i^g),\ 1 \le j \le N_c, 1 \le i \le M$, respectively; and $\underline{x}_M^g = [x_1^g \ldots x_M^g] \in \mathbb{R}^M$ is the set of interpolation points.

Finally, we evaluate the output estimates from

$$s_{1,N,M}^k(\mu) = L_{T,N}^T\, \underline{T}_{N,M}^k(\mu) + 1, \quad \forall\, k \in \mathbb{K}, \quad (61)$$

and

$$s_{2,N,M}^k(\mu) = L_{c,N}^T\, \underline{c}_{N,M}^k(\mu) + 1, \quad \forall\, k \in \mathbb{K}, \quad (62)$$

where $L_{T,N} = (Z_T)^T L_T \in \mathbb{R}^{N_T}$ and $L_{c,N} = (Z_c)^T L_c \in \mathbb{R}^{N_c}$ are the output vectors.

The online-offline decomposition is now clear. In the offline stage — performed only once — we first construct the nested approximation space W_M^g and sets of interpolation points T_M^g, $1 \le M \le M_{\max}$; we then generate the reduced basis spaces $W_{N_T}^T$ and $W_{N_c}^c$ for temperature and concentration, respectively; and finally we store the parameter independent quantities $M_{T,N}$, $A_{T,N}$, $D_T^{M,N}$, $M_{c,N}$, $A_{c,N}$, $D_c^{M,N}$, $Z_T^{M,N}$, $Z_c^{M,N}$, and B^M. In the online stage — given a new parameter value μ — we solve (59) and (60) for $\underline{T}_{N,M}^k(\mu)$ and $\underline{c}_{N,M}^k(\mu)$ and evaluate the outputs $s_{1,N,M}^k(\mu)$ and $s_{2,N,M}^k(\mu)$ from (61) and (62), respectively. The operation count in the online stage is $O(MN^2 + N^3)$ per Newton step per timestep, where $N = N_T + N_c$. The operation count in the online stage is thus *independent* of $\mathcal{N}$.

4. Numerical Results

We now present numerical results for the model problem introduced in Section 3.1. We choose for $\Xi_{\text{train}} \subset \mathcal{D}$ a regular grid of 15 parameter points over $\mathcal{D}$ and we take $\mu_1^g = 12$. Next, we pursue the POD/Greedy-EIM procedure to construct W_M^g, T_M^g, and B^M, $1 \le M \le M_{\max}$, with $M_{\max} = 36$. We plot the convergence of $\varepsilon_{M,\max}^g$ in Figure 7.

We next turn to the reduced basis approximation and construct the reduced basis spaces $W_{N_T}^T$ and $W_{N_c}^c$ according to the adaptive sampling procedure outlined in Section 2.3.3 using the train sample Ξ_{train}. In Figure 8(a) and (b) we plot, as a function of N_T, N_c, and M, the maximum relative errors $\epsilon_{N,M,\text{max,rel}}^T$ in the temperature and $\epsilon_{N,M,\text{max,rel}}^c$ in the concentration, respectively; here $\epsilon_{N,M,\text{max,rel}}^T = \max_{\mu\in\Xi_{\text{Test}}} |||T^K(\mu) - T_{N,M}^K(\mu)|||/|||T^K(\mu_T)|||$, where $\mu_T \equiv \arg\max_{\mu\in\Xi_{\text{Test}}} |||T^K(\mu)|||$ (similarly for $\epsilon_{N,M,\text{max,rel}}^c$) and Ξ_{Test} is

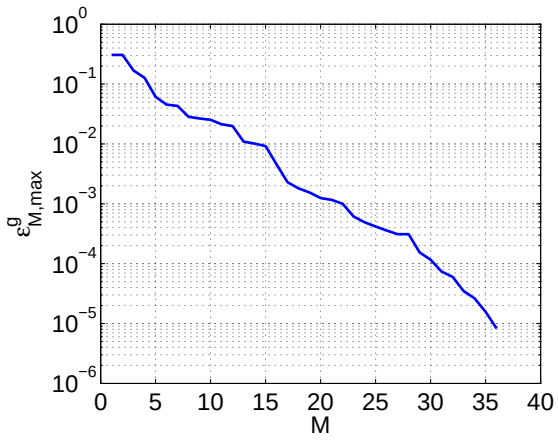

Figure 7: Convergence results for EIM interpolation error.

a test sample of size 25 (a regular grid in $\mathcal{D}$; note that the test and train samples are, of course, different). We observe that the reduced basis approximation converges very rapidly. We also note the "plateau" in the curves for M fixed and the "drops" in the $N_T, N_c \to \infty$ asymptotes as M increases: for fixed M the error due to the coefficient function approximation will ultimately dominate for large N_T and N_c; increasing M renders the coefficient function approximation more accurate, which in turn leads to a drop in the error. We further note that the separation points, or "knees," of the N_T-M-convergence curves (resp. N_c-M-convergence curves) reflect a balanced contribution of both error terms; neither N_T (resp. N_c) nor M limit the convergence of the reduced basis approximation.

We next turn to the output estimate and present, in Figure 9(a) and (b), as a function of N_T, N_c, the maximum relative output errors $\epsilon^{s1}_{N,M,\max,\mathrm{rel}}$ and $\epsilon^{s2}_{N,M,\max,\mathrm{rel}}$, respectively; here, $\epsilon^{s}_{N,M,\max,\mathrm{rel}}$ is the maximum over Ξ_{Test} of $|s(t_s^k(\mu);\mu) - s_{N,M}(t_s^k(\mu);\mu)|/|s(t_s^k(\mu);\mu)|$, where $t_s^k(\mu) \equiv \arg\max_{k\in\mathbb{K}} |s^k(\mu)|$.

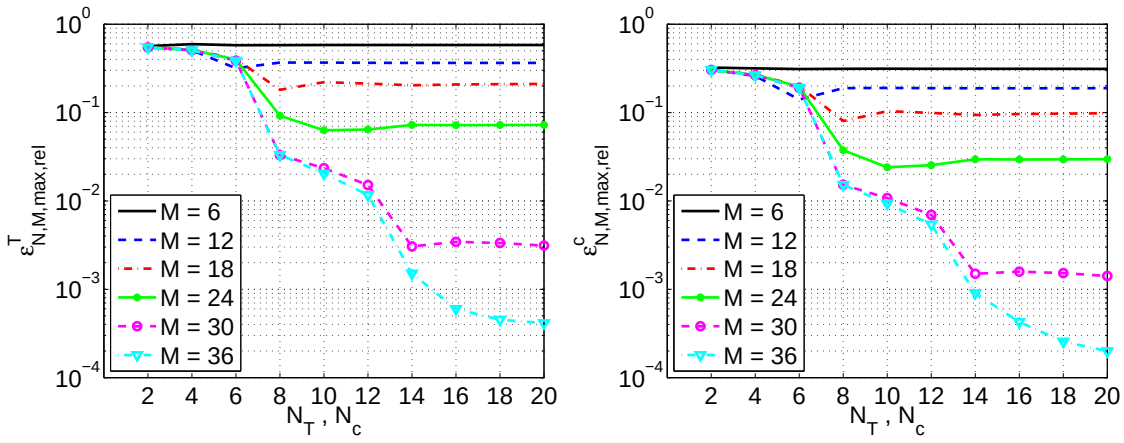

(a) (b)

Figure 8: Convergence of the reduced basis approximation: maximum relative error in the energy norm.

We observe also very rapid convergence of the reduced basis output approximation. The output error shows the same behavior as the error in the energy norm: the M-asymptotes level off at a lower and lower error as M increases. To obtain a maximum relative error in both outputs of less than 1%, we require approximately $M = 30$, $N_T = 13$, and $N_c = 13$.

In Table 1 we present, as a function of $N = N_T = N_c$ and M, the average online computational times to calculate $s^k_{1,N,M}(\mu)$ and $s^k_{2,N,M}(\mu)$ for all $k \in \mathbb{K}$ and for all $\mu \in \Xi_{\text{Test}}$. The values are normalized with respect to the computational time for the direct calculation of the truth approximation output $s^k_1(\mu)$ and $s^k_2(\mu)$ for all $k \in \mathbb{K}$. The computational savings are $O(100)$ for all values of $N = N_T = N_c$ and M. For an accuracy of less than 1% in the output bound ($N_T = N_c = 13$, $M = 30$) the computational savings are approximately a factor of 300.

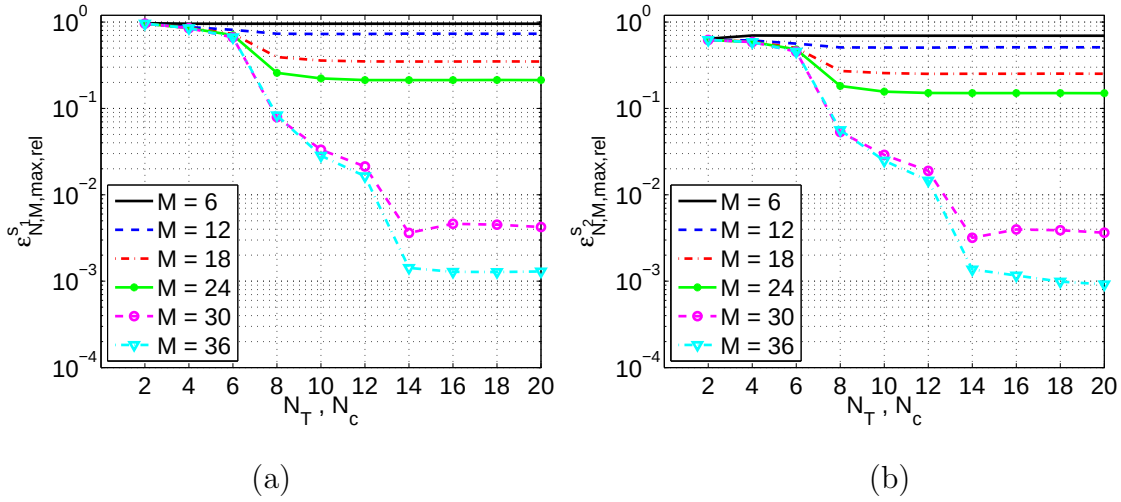

Figure 9: Convergence of the reduced basis approximation: maximum relative output error.

Finally, we present in Figure 10 the truth temperature output $s_1^k(\mu)$, the reduced basis output approximation $s_{1,N,M}^k(\mu)$ and the relative error $|s_1^k(\mu) - s_{1,N,M}^k(\mu)|/s_{1,\max}(\mu)$ as a function of (discrete) time for $\mu = 12.6$; here, $s_{1,\max}(\mu) = \max_{k\in\mathbb{K}} s_1^k(\mu)$. The corresponding results for the concentration output are shown in Figure 11. Note that $\mu = 12.6$ is the most difficult parameter value in terms of dynamic behaviour due to the highest temperature during ignition and the following mixed mode oscillation. The reduced basis approximation reproduces the the initial ignition as well as the mixed mode oscillation very well. The maximum relative error (shown on a log-scale) remains approximately on the order of 10^{-4} throughout the whole time interval of interest.

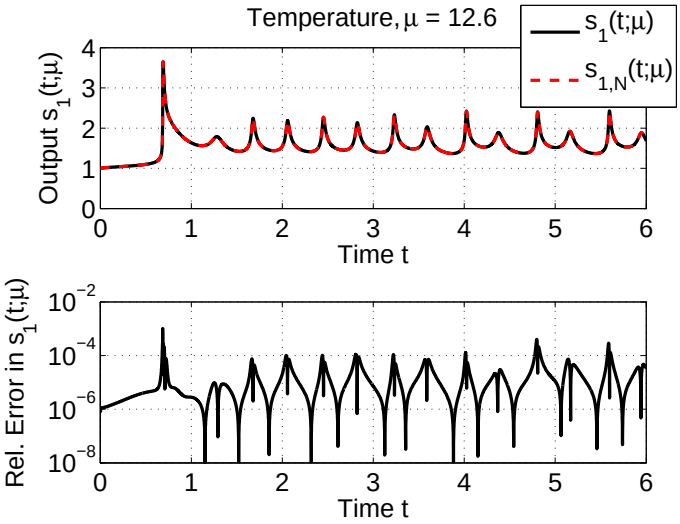

Figure 10: Output $s_1(t;\mu)$, output estimate $s_{1,N,M}(t;\mu)$, and relative output error as a function of time for $\mu = 12.6$ and $N =$ and $M =$.

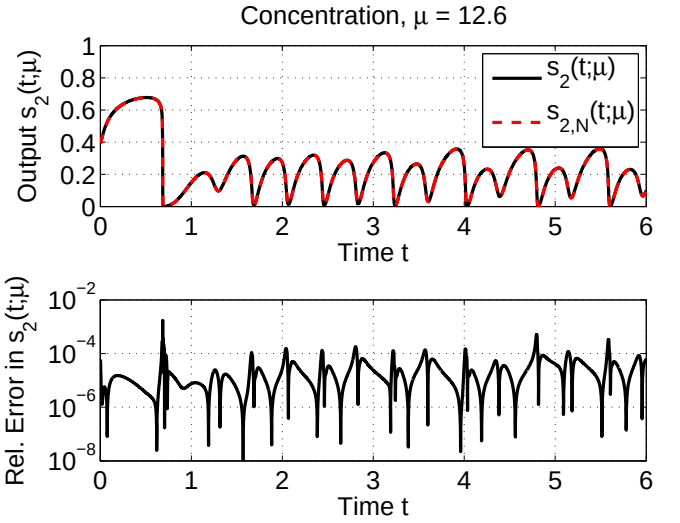

Figure 11: Output $s_2(t;\mu)$, output estimate $s_{2,N}(t;\mu)$, and relative output error as a function of time for $\mu = 12.6$.

N	M	$s^k_{1/2,N,M}(\mu),\ \forall k \in \mathbb{K}$	$s^k_{1/2}(\mu),\ \forall k \in \mathbb{K}$
4	12	2.22 E – 03	1
8	30	2.74 E – 03	1
12	30	3.42 E – 03	1
16	36	3.96 E – 03	1
20	36	5.12 E – 03	1

Table 1: Online computational times to solve for $s^k_{1/2,N,M}(\mu)$ normalized with respect to the time to solve for $s^k_{1/2}(\mu)$ for $1 \leq k \leq K$.

5. Conclusions

We have presented a model order reduction technique for parametrized nonlinear reaction-diffusion systems. To this end, we employed the reduced basis method, a model order reduction technique which proved very powerful for systems with simultaneous dependence on parameter and time. We presented numerical results for a nonlinear reaction-diffusion system modelling the self-ignition of a coal stockpile. The reduced basis approximation converged very fast – despite the complex dynamic behaviour and strong dependence on the parameter – resulting in a significant dimension reduction. Although we only considered the Arrhenius number as a system parameter, the methodology presented directly applies to the remaining physical parameters. Thus, problems with a dependence on multiple parameters *and* time pose no impediment for our approach. Note that the methodology can also be extended to treat geometric parametrizations (Rozza et al., 2008).

Our second focus was the development of an efficient offline-online computational procedure even in the presence of strong nonlinearities. To this

end, we employed the empirical interpolation method to construct an affine coefficient-function approximation of the nonlinear term. The EIM allows a complete decoupling of the offline stage — where the reduced basis spaces are generated — and the online stage — where, given a new parameter value, we solve the reduced basis approximation and evaluate the output. The online stage depends only on N and M and the parametric complexity of the problem. We observed a significant $O(10^2)$ reduction in online computational time for the solution of the reduced model compared to the solution of the full model.

We thus believe that if there is a high premium on *real-time* performance or a *many-query* context — for example in the design, optimization, control, and characterization contexts — the reduced basis approach presented here can be very gainfully employed.

Acknowledgements

I would like to thank Professor Anthony T. Patera of MIT for many fruitful discussions. This work was supported by the Excellence Initiative of the German federal and state governments.

References

Adjerid, S., & Flaherty, J. E. (1986). A moving finite element method with error estimation and refinement for one-dimensional time dependent partial differential equations. *SIAM Journal on Numerical Analysis*, *23*, pp. 778–796.

Astrid, P. (2004). Fast reduced order modeling technique for large scale ltv systems. In *Proceedings of the 2004 American Control Conference* (pp. 762 – 767). Boston, MA volume 2.

Balsa-Canto, E., Alonso, A., & Banga, J. (2004). Reduced-order models for nonlinear distributed process systems and their application in dynamic optimization. *Ind. Eng. Chem. Res.*, *43*, 3353–3363.

Barrault, M., Nguyen, N. C., Maday, Y., & Patera, A. T. (2004). An "empirical interpolation" method: Application to efficient reduced-basis discretization of partial differential equations. *C. R. Acad. Sci. Paris, Série I.*, *339*, 667–672.

Brooks, K., Balakotaiah, V., & Luss, D. (1988a). Effect of natural convection on spontaneous combustion of coal stockpiles. *AIChE Journal*, *34*, 353–365.

Brooks, K., Bradshaw, S., & Glasser, D. (1988b). Spontaneous combustion of coal stockpiles - an unusual chemical reaction engineering problem. *Chemical Engineering Science*, *43*, 2139 – 2145.

Brooks, K., & Glasser, D. (1986). A simplified model of spontaneous combustion in coal stockpiles. *Fuel*, *65*, 1035 – 1041.

Bui, T., Damodaran, M., & Wilcox, K. (2003). Proper orthogonal decomposition extensions for parametric applications in transonic aerodynamics (AIAA Paper 2003-4213). In *Proceedings of the 15th AIAA Computational Fluid Dynamics Conference*.

Chaturantabut, S., & Sorensen, D. C. (2010). Nonlinear model reduction via discrete empirical interpolation. *SIAM Journal on Scientific Computing*, *32*, 2737–2764.

Christensen, E., Brøns, M., & Sørensen, J. (2000). Evaluation of proper orthogonal decomposition-based decomposition techniques applied to parameter-dependent nonturbulent flows. *SIAM J. Scientific Computing*, *21*, 1419–1434.

Christofides, P. (2001a). Control of nonlinear distributed process systems: Recent developments and challenges. *AIChE Journal*, *47*, 514–518.

Christofides, P. (2001b). *Nonlinear and Robust Control of PDE Systems*. Birkhäuser.

Daniel, L., Ong, C. S., Low, S. C., Lee, K. H., & White, J. (2002). Geometrically parameterized interconnect performance models for interconnect synthesis. In *in Proceedings of 2002 International Symposium on Physical Design, 2002* (pp. 202–207).

Eftang, J., Grepl, M., & Patera, A. (2010). A posteriori error bounds for the empirical interpolation method. *C. R. Acad. Sci. Paris, Ser. I*, *348*, 575–579.

Grepl, M. (2005). *Reduced-Basis Approximation and A Posteriori Error Estimation for Parabolic Partial Differential Equations*. Ph.D. thesis Massachusetts Institute of Technology.

Grepl, M. (submitted, 2010). A posteriori error bounds for reduced basis

approximations of nonaffine and nonlinear parabolic partial differential equations. *M3AS*, .

Grepl, M., Maday, Y., Nguyen, N., & Patera, A. (2007). Efficient reduced-basis treatment of nonaffine and nonlinear partial differential equations. *ESAIM: M2AN*, *41*, 575–605.

Grepl, M., & Patera, A. (2005). A posteriori error bounds for reduced-basis approximations of parametrized parabolic partial differential equations. *ESAIM: M2AN*, *39*, 157–181.

Gunzburger, M. D., Peterson, J. S., & Shadid, J. N. (2007). Reduced-order modeling of time-dependent pdes with multiple parameters in the boundary data. *Computer Methods in Applied Mechanics and Engineering*, *196*, 1030 – 1047.

Haasdonk, B., & Ohlberger, M. (2008). Reduced basis method for finite volume approximations of parametrized linear evolution equations. *ESAIM: M2AN*, *42*, 277–302.

Hahn, J., & Edgar, T. (2002). An improved method for nonlinear model reduction using balancing of empirical gramians. *Computers and Chemical Engineering*, *26*, 1379–1397.

Holmes, P., Lumley, J., & Berkooz, G. (1996). *Turbulence, coherent structures, dynamical systems and symmetry*. Cambridge University Press.

Kapila, A. (1983). *Asymptotic treatment of chemically reacting systems*. Elsevier Science Pub. Co. Inc.,New York, NY.

Knezevic, D., Nguyen, N., & Patera, A. (submitted 2009). Reduced basis approximation and a posteriori error estimation for the parametrized unsteady Boussinesq equations. *Mathematical Models and Methods in Applied Sciences*, .

Lall, S., Marsden, J., & Glavaski, S. (1999). Empirical model reduction of controlled nonlinear sytems. In *Proceedings of the 14th IFAC world congress*. Beijing, China.

Lall, S., Marsden, J. E., & Glavaski, S. (2002). A subspace approach to balanced truncation for model reduction of nonlinear control systems. *Int. J. Robust Nonlinear Control*, *12*, 519–535.

Maday, Y., Nguyen, N., Patera, A., & Pau, S. (2009). A general multipurpose interpolation procedure: The magic points. *Communications on Pure and Applied Analysis (CPAA)*, *8*, 383–404.

Marquardt, W. (2002). Nonlinear model reduction for optimization based control of transient chemical processes. In *Proceedings of the 6th International Conference on Chemical Process Control* (pp. 12–42). volume 98 of *AIChe Symp. Ser.326*.

Moore, B. (1981). Principal component analysis in linear systems: Controllability, observability, and model reduction. *IEEE Transactions on Automatic Control*, *26*, 17–32.

Nguyen, N., Rozza, G., & Patera, A. (2009). Reduced basis approximation and a posteriori error estimation for the time-dependent viscous burgers' equation. *Calcolo*, *46*, 157–185.

Prud'homme, C., Rovas, D., Veroy, K., Maday, Y., Patera, A. T., & Turinici, G. (2002). Reliable real-time solution of parametrized partial differential equations: Reduced-basis output bound methods. *Journal of Fluids Engineering*, *124*, 70–80.

Rathinam, M., & Petzold, L. (2003). A new look at proper orthogonal decomposition. *SIAM J. Numer. Anal*, *41*, 1893–1925.

Romijn, R., Özkan, L., Weiland, S., Ludlage, J., & Marquardt, W. (2008). A grey-box modeling approach for the reduction of nonlinear systems. *Journal of Process Control*, *18*, 906–914.

Rowley, C. (2005). Model reduction for fluids using balanced proper orthogonal decomposition. *International Journal of Bifurcation and Chaos*, *15*, 997–1013.

Rozza, G., Huynh, D., & Patera, A. (2008). Reduced basis approximation and a posteriori error estimation of affinely parametrized elliptic coercive partial differential equations. *Archives of Computational Methods in Engineering*, *15*, 229–275.

Salinger, A., Aris, R., & Derby, J. (1994). Modeling the spontaneous ignition of coal stockpiles. *AIChE Journal*, *40*, 991–1004.

Schmal, D., Duyzer, J., & van Heuven, J. (1985). A model for the spontaneous heating of coal. *Fuel*, *64*, 963–972.

Shvartsman, S., & Kevrekidis, I. (1998). Nonlinear model reduction for control of distributed systems: A computer-assisted study. *AIChE Journal*, *44*, 1579–1595.

Shvartsman, S. Y., Theodoropoulos, C., Rico-Martnez, R., Kevrekidis, I. G., Titi, E. S., & Mountziaris, T. J. (2000). Order reduction for nonlinear dynamic models of distributed reacting systems. *Journal of Process Control*, *10*, 177 – 184.

Sirovich, L. (1987). Turbulence and the dynamics of coherent structures, part 1: Coherent structures. *Quarterly of Applied Mathematics*, *45*, 561–571.

Sirovich, L., & Kirby, M. (1987). Low-dimensional procedure for the characterization of human faces. *Journal of the Optical Society of America A*, *4*, 519–524.

Smoller, J. (1994). *Shock Waves and Reaction-Diffusion Equations*. Springer.

Veroy, K., & Patera, A. T. (2005). Certified real-time solution of the parametrized steady incompressible Navier-Stokes equations; Rigorous reduced-basis *a posteriori* error bounds. *International Journal for Numerical Methods in Fluids*, *47*, 773–788.

Veroy, K., Prud'homme, C., & Patera, A. T. (2003). Reduced-basis approximation of the viscous Burgers equation: Rigorous *a posteriori* error bounds. *C. R. Acad. Sci. Paris, Série I*, *337*, 619–624.

Willcox, K., & Peraire, J. (2001). Balanced model reduction via the proper orthogonal decomposition. In *15th AIAA Computational Fluid Dynamics Conference*. AIAA.